



Ni foam as the current collector for high capacity C–Si composite electrode

Qina Sa, Yan Wang*

Department of Mechanical Engineering, Worcester Polytechnic Institute, 100 Institute Road, MA 01609, United States

ARTICLE INFO

Article history:

Received 9 December 2011

Received in revised form 6 February 2012

Accepted 6 February 2012

Available online 13 February 2012

Keywords:

Ni foam

Cu foil

Current collector

Si electrode

Lithium ion batteries

ABSTRACT

Si electrode is very promising as the anode material for next generation lithium ion batteries requiring high capacity and energy because of its high theoretical capacity (4200 mAh g^{-1} compared to 372 mAh g^{-1} for graphite) and low discharge potential ($\sim 0.5 \text{ V vs. Li/Li}^+$). However, fast capacity fading of Si electrode is suffered from huge volume expansion and contraction during charging and discharging. Although many methods, including nanostructured electrode, thin film and composite electrode, have been proposed to overcome the capacity fading problem, high synthesis cost and/or poor effects prevent them from being used in the commercial applications. In this study, 3-dimensional (3D) Ni foam is adopted as the current collector for high capacity C–Si composite electrode. The results show that Ni foam can effectively suppress the electrode expansion and greatly improve the cycle life of Si electrode due to the 3D structure. Electrochemical impedance spectroscopy also shows that the electrode with Ni foam show much lower impedance after cycling. Therefore, adopting Ni foam as the current collector provides a new way to incorporate the electrode materials with large volume expansion.

© 2012 Elsevier B.V. All rights reserved.

1. Introduction

Lithium ion batteries are now being developed rapidly and used widely because of their high energy density, power density and long cycle life compared to other battery technologies. However, with the development of personnel electronics, hybrid and electric vehicles, lithium ion batteries with even higher capacity and energy density need to be developed. To improve the performance of lithium ion batteries, various active materials have been researched. Among all the anode materials, graphite anode suffers from low reversible capacity and irreversible capacity loss [1], lithium alloys have the disadvantage of potential safety and loss of capacity [2–5], and silicon is the most favorable material because of its high theoretical specific capacity (4200 mAh g^{-1} based on the formation of $\text{Li}_{4.4}\text{Si}$ phase) and low discharge potential ($\sim 0.5 \text{ V vs. Li/Li}^+$) [6]. However, the huge volume expansion (300%) for Si electrode limits its practical application in lithium ion batteries [7]. The stress induced by volume changes causes cracking and pulverization of Si anode and Si particles can lose electronic contact with each other and the current collector, which results in fast fading [8,9].

In order to overcome the volume expansion problem, several approaches have been proposed. One approach is to use 3D Si nanowire or nanotube, which is commonly deposited onto a sub-

strate by a chemical vapor deposition (CVD) method [10–13]. Si nanowires of small diameter better accommodate of large volume changes and the 1D geometry provides an efficient electronic charge transport pathway. Although results from nanowire-based electrodes are promising, high synthesis cost can prevent their adoption by industry. The main alternative approach is to use a C–Si composite to overcome the volume expansion problem [14]. However, the large volume changes in Si on Li insertion can be accommodated by carbon only to a limited degree, thus offering limited stability and cycle life. There is also some research work on Si thin film with or without coatings [15]. Although Si thin film showed improved cycle life, it still cannot meet practical requirement for industrial applications. Kovalenko et al. [16] has utilized alginate as the binder with nano-Si to fabricate the electrodes for lithium ion batteries and very stable and high capacity has been obtained in their recent report.

Throughout the research of lithium ion batteries, much effort has been devoted into the development of new cathode and anode materials. Except for the electrode material, current collector is also playing an extremely important role in the rechargeable lithium ion battery. Its physical and chemical properties can impact the performance of lithium ion batteries. Different current collectors can result in significant difference on the performances of the lithium ion batteries. Normally, copper foil [17,18] is utilized as anode current collector and aluminum foil for the cathode in the conventional lithium ion batteries.

Nickel foam is the current collector of cathode materials in Ni/MH batteries [19] and the thickness of nickel foam is $\sim 0.7 \text{ mm}$

* Corresponding author. Tel.: +1 508 831 5453; fax: +1 508 831 5178.
E-mail address: yanwang@wpi.edu (Y. Wang).

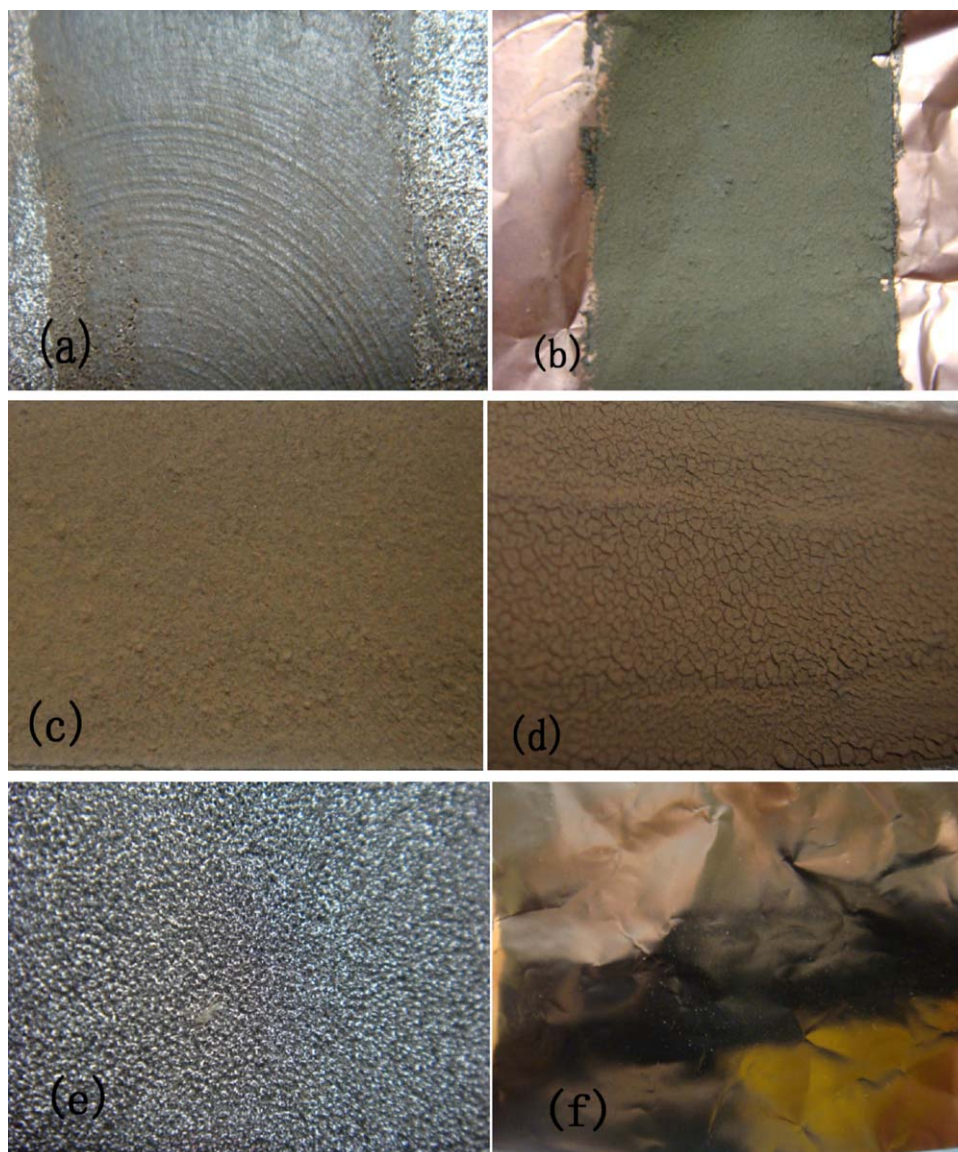


Fig. 1. (a) 20 wt% Si anode on Ni foam current collector. (b) 20 wt% Si anode on Cu foil current collector. (c) 40 wt% Si anode on Ni foam current collector. (d) 40 wt% Si anode on Cu foil current collector. (e) Ni foam current collector. (f) Cu current collector.

and the porosity is in the range of 50–95%. The 3D structure has the ability to incorporate the active materials into the current collector, not on the surface. In this study, nickel foam is applied as anode current collector for high capacity Si electrode of lithium ion batteries, and the rate capacities and cycle life of different weight percent silicon electrodes are examined. It is showing that the cycle life of Si electrode was greatly improved with nickel foam as the current collector compared to the conventional copper current collector. The volume expansion effect is significantly reduced because of the network geometry of nickel foam.

2. Experimental

2.1. Electrode preparation

The anode C–Si was prepared by the typical procedure of mixing the electro-active silicon and graphite powders with conductive carbon and the binder, and then the slurry was casted on the Cu (0.025 mm thick, purchased from MTI) or Ni (Hunan Curun, China) current collectors and dried and pressed. Initial thickness of Ni foam

is 0.75 mm and the porosity is about 90%. Before being used as current collector, Nickel foam was pressed to 0.2 mm thick. Then a small piece of electrode was punched from the dried product, each electrode was 0.153 cm² and 1.3 mg. Swagelok cells were assembled in glove box which is filled with argon gas. 1 M LiPF₆ dissolved in EC + DMC + DEC (1:1:1 in volume) was used as electrolyte. The ingredient of electrode included 10 wt% of binder and 10 wt% of conductive carbon, and the rest 80 wt% was occupied by silicon (Alfa Aesar, APS < = 50 nm, 98% purity) and graphite powders. The binder was prepared by 2.5 wt% poly(vinylidene fluorides) (PVDF) dissolved in N-Methyl-2-Pyrrolidone (NMP) solvent. The electrodes of 20 wt% and 40 wt% of silicon were tested utilizing nickel and copper as current collectors, respectively. The surface morphology was characterized using JSM-7000F Scanning electron microscopy.

2.2. Electrochemical testing

For the electrochemical tests, VMP3 from Biological Instrument was used. Electrochemical cells were charged at constant current constant voltage (CCCV) and discharged at constant cur-



Fig. 2. The comparison of the anodes on Cu foil (left) and Ni foam (right) after cycling.

rent (CC) with different rates in $-1.5-0\text{V}$ voltage range. For cycle tests, the cell was charged and discharged at $C/15$. Electrochemical impedance spectroscopy (EIS) measurements were performed at open circuit potential with discharged states after cycling and the perturbation amplitude was 10mV . All cells were tested at room temperature.

3. Results and discussion

3.1. Physical properties of anode materials on Ni and Cu current collectors

$20\text{wt}\%$ and $40\text{wt}\%$ Si anode were casted on Ni and Cu substrates. After dried for 20h , it was observed that there were extensive cracks on $40\text{wt}\%$ Si anode on Cu substrate (Fig. 1d) and the active materials on Cu substrate were very easily dropped off and the product was unable to be utilized as electrode to assemble cells. Cu foil is very flat and no complicated structure, the only space for the electrode materials is on the surface. When the electrode is dried or after cycled, there is no flexible room for the adjustment of the volume change of the electrode. That is why there are so many cracks and the existence of the extra edge of the electrode based on Cu foil. Contrary to that, the electrodes casted on Ni foam were surprisingly evenly covered both for $20\text{wt}\%$ and $40\text{wt}\%$ Si and no apparent cracks appeared (Fig. 1a and c). It is noticeable that the surface of Cu foil is too smooth (Fig. 1f) compared to the network geometry of Ni foam (Fig. 1e) can provide much more flexible space for the anode to spread or self-adjusted during casting process.

Also, it should be pointed out that the particular geometry of Ni foam current collector also helps reduce the volume expansion effect of Si. Fig. 2 shows the back side of electrodes with Cu and Ni current collectors after about 90 cycles. It can be clearly recognized that the anode on Cu had already exceeded the edge of Cu foil and the area of Cu could not hold the extended electrode any more, which can lead to the bad connection between electrode and current collector. Also, part of the electrode has dropped off from the Cu foil. However, by the presence of Ni foam, the volume extension after cycling did not influence the Si/Ni combination and the electrode still located within the area of Ni. It is revealed that the pores of the network structure offer extra space for Si volume extension.

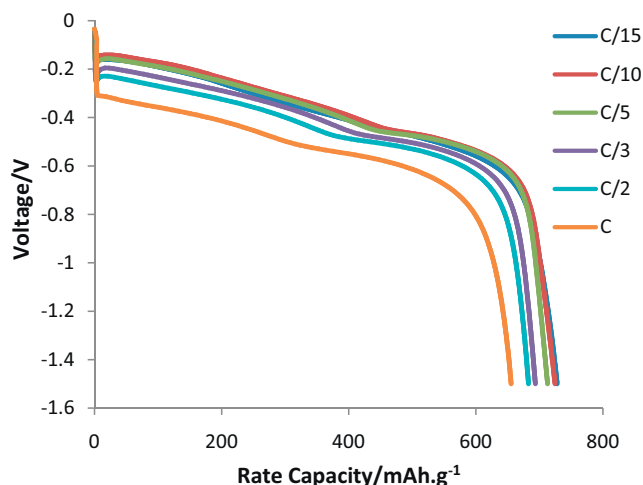


Fig. 3. Rate capacity of $20\text{wt}\%$ Si on Cu foil.

3.2. Rate performance of Si anode on Ni and Cu current collectors

Figs. 3–6 show the electrochemical discharge rate capacity performance of the Si anode on Ni and Cu current collectors. The data of rate capacity of $C/15$, $C/10$, $C/5$, $C/3$, $C/2$ and $C/1$ for each case was obtained and analyzed. With increasing the discharge rate, the capacity decreases. The electrode with $40\text{wt}\%$ Si on Ni has the highest rate capacity at $C/15$ because of the high capacity of Si. However, as the current increases, the capacity decreases significantly to 143mAh g^{-1} at 1C . The capacity of $20\text{wt}\%$ Si on Ni at 1C is 473mAh g^{-1} , which is much higher than that of $40\text{wt}\%$ Si anode. Also, it can be seen that the 6 curves of $40\text{wt}\%$ Si on Ni rate capacity appears to have much more difference compared to those of $20\text{wt}\%$ Si, showing the rate capacity drops fast when the amount of silicon is increased. This can be explained by the more volume change associated with high percentage of Si.

A rate capacity of 724mAh g^{-1} was obtained at $C/15$ of Si anode on Cu current collector, and that of $20\text{wt}\%$ Si on Ni is 643mAh g^{-1} . It is known that Si anode on Cu shows good results at rate capacity test, and it works well even at high current. The reason is that the electrical contact between Cu foil and testing cell is better than the nickel foam. Unlike Cu substrate, the contact area between Ni foam with high porosity with the testing cell is much smaller than that

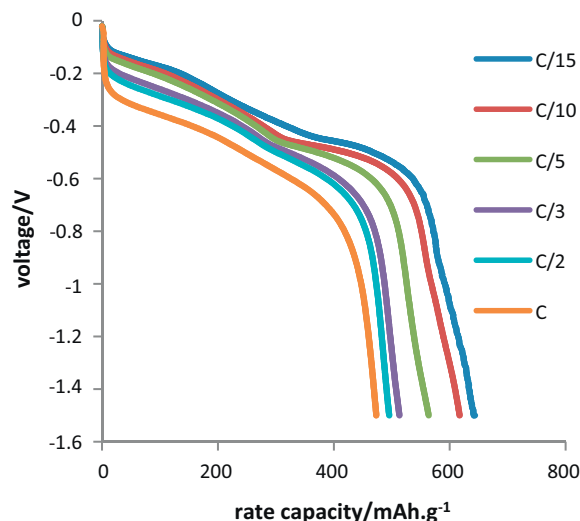


Fig. 4. Rate capacity of $20\text{wt}\%$ Si on Ni foam.

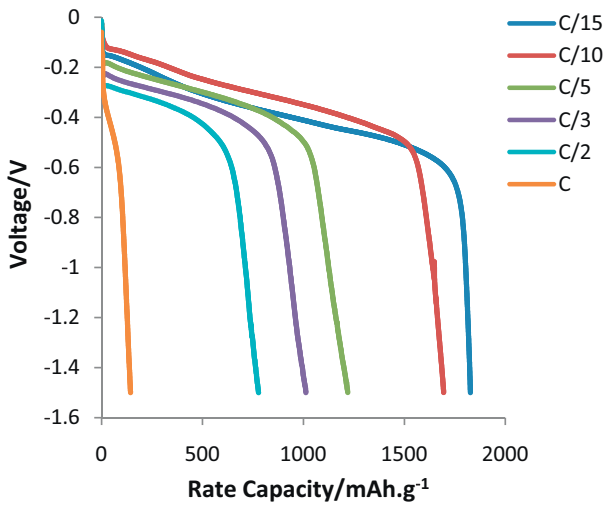


Fig. 5. Rate capacity of 40 wt% Si on Ni foam.

of Cu substrate. Also, from Fig. 6 we can see that the relative specific rate capacity of Si anode on Cu shows better performance, the specific rate capacity of 40 wt% Si on Ni decreased rapidly because of the existence of much more Si.

However, as shown in previous section, such Cu foil is not capable of higher weight percent of Si due to cracks and the capacity of the lower weight percent Si anode is limited. Its capacity at C/15 is much lower than that of 40 wt% Si on Ni. On the other hand, acceptable rate capacity is not the only factor to evaluate the quality of an electrode or battery, a longer cycle life, is even more important for a reliable battery design. A long cycle life battery can save the resources and expense of production process. Cu can only display good results at the very beginning of cycle life. As the charge and discharge process continues, Si on Ni current collector will show advantage of long cycle life. This will be discussed in next section.

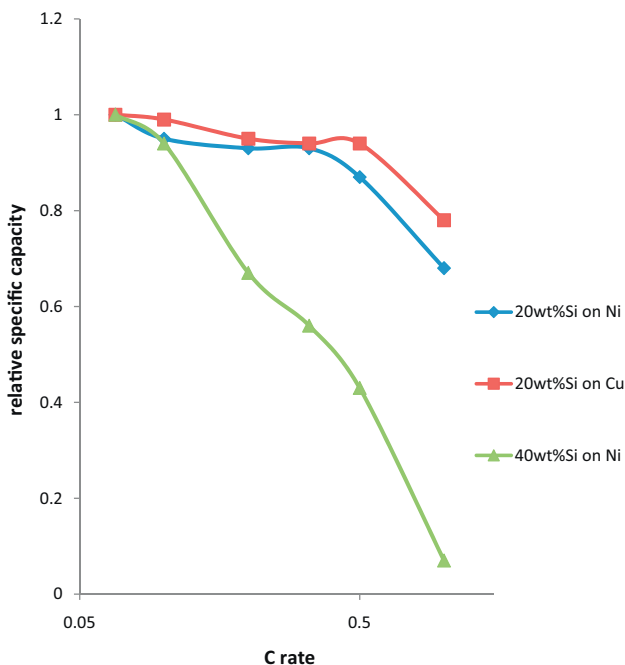


Fig. 6. Specific rate capacity of the three anodes on Ni and Cu current collectors.

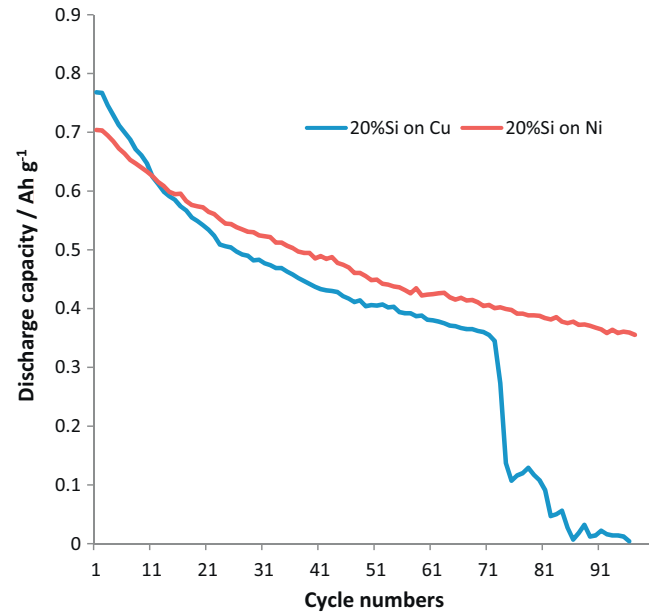


Fig. 7. Cycle life comparison of 20 wt% Si on Ni and 20 wt% Si on Cu.

3.3. Cycle life of Si anode on Ni and Cu current collectors

The cycle life of both 20 wt% and 40 wt% of Si on Ni current collectors and 20 wt% of Si on Cu was examined. Fig. 7 is a comparison of anode based on Ni and Cu current collectors. All the cycles were conducted at C/15 charge and discharge. We can clearly see that at the beginning of cycle test, anode on Cu foil shows good performance and started from a discharge capacity of 768 mAh g⁻¹. However, after 70 cycles, the electrode with Cu current collector started to fade significantly and the capacity decreased to a very small value. The reason is that active materials have lost good connection with Cu substrate, which will significantly increase the impedance of the cell, lower the charge and discharge efficiency. The data in Fig. 7 suggests the crucial role of the Ni current collector, and its network

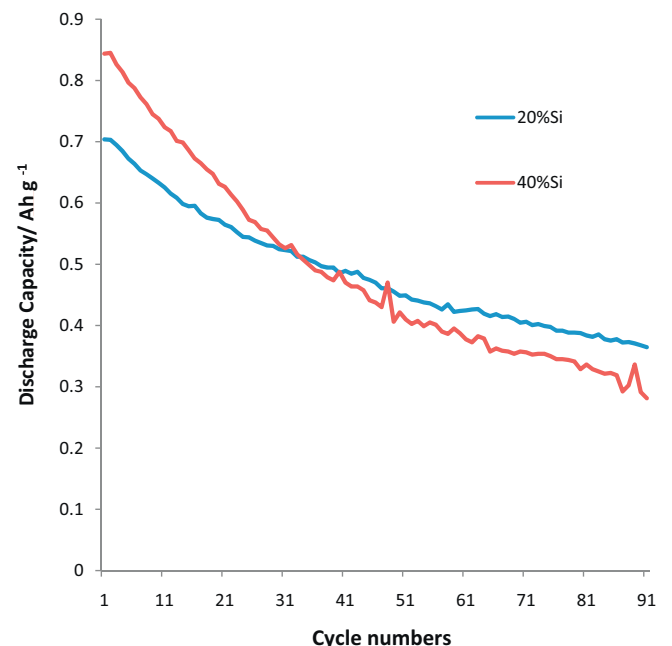


Fig. 8. Cycle life comparison of 20 wt% Si and 40 wt% Si on Ni.

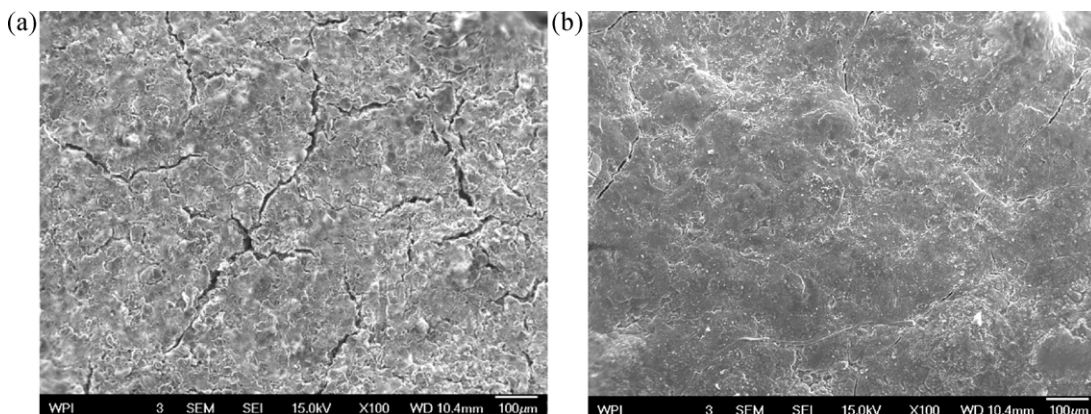


Fig. 9. SEM images of 20 wt% Si on Ni, (a) before cycling and (b) after cycling.

geometry can effectively prevent the Si anode from fading rapidly. The Ni current collector of 20 wt% Si starts from a discharge capacity of 700 mAh g^{-1} , slightly smaller than that of anode on Cu. But the 20 wt% Si on Ni ends up with a 350 mAh g^{-1} capacity when the 20 wt% Si on Cu is almost 0 after 95 cycles.

20 wt% and 40 wt% Si anode were tested for 90 cycles. Si is known to have a very high capacity of 4200 mAh g^{-1} , so more Si was added in the anode, the higher capacity the anode achieves. However, on the other hand, the more Si was added, the more significant volume extension will be going on and the capacity will fade faster. This is proved by the cycle life of the two anodes containing different amounts of Si. As shown in Fig. 8, at the beginning of cycles, the electrode with 40 wt% Si has a much higher capacity, but the slope of 20 wt% Si anode graph is much smaller than that of 40 wt% Si, which presents the 20 wt% one has a slower fading rate. The capacity of 40 wt% Si is fading so fast that after about 43 cycles, 20 wt% Si anode has a higher capacity than that of 40 wt%. But it can be seen from the figure that the difference between 20 wt% and 40 wt% Si on Ni is not that huge, even for 40 wt% Si, the cycle life on Ni is still better than that of Cu based electrode. At this point, the Ni current collector does improve the cycle life significantly. Besides that, the coulombic efficiencies of Si on Ni and Cu are examined, both of them are performing an average of 97% efficiency, which is indicating that the Ni foam current collector can provide improved cycle life as well as good coulombic efficiency.

Fig. 9 displays the SEM images before and after cycling of the anodes on Ni current collectors. The surface of anode was enlarged to 100 times larger. Interestingly, it is shown that the amount of cracks on the surface of after-cycled anode is much less than that of before-cycled anode. It is possible that after cycling the total volume of electrode was enlarged because of the volume expansion of Si and the cracks were filled.

3.4. Electrochemical impedance performance of Si anode on Ni and Cu current collectors

After the cycle life test of the different weight percent Si anodes on Ni foam and Cu foil, electrochemical impedance spectroscopy was examined. Fig. 10 shows the electrochemical impedance spectra of 20 wt% Si on Ni and Cu current collectors as well as the 40 wt% Si based on Ni foam. To maintain uniformly, all the cells were test under the discharged state (state of discharge 100%). In the spectra, one semicircle and one straight line were observed for all three curves. However, if we compare the three curves, the impedance of the semicircle of the electrode with Cu foil as the current collector is around $40,000 \Omega$ when being extended to the x-axis. The impedance of the semicircle of the electrode with Ni foam as the current collector is only around 1000Ω . These differences suggest

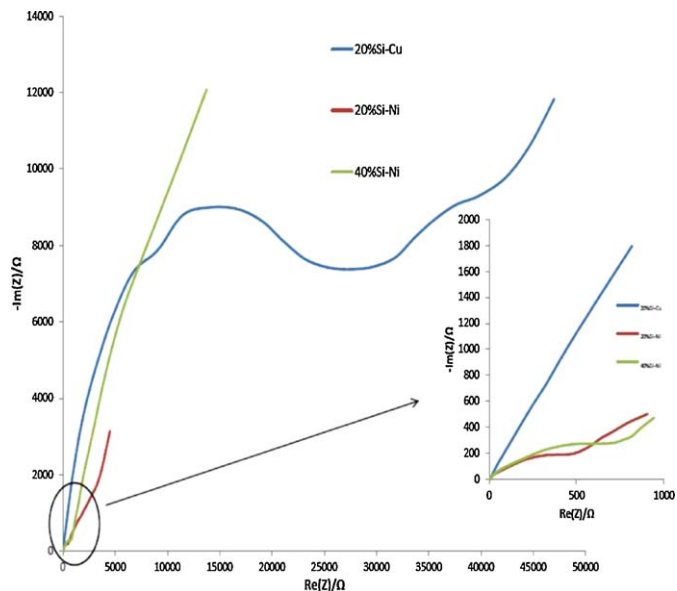


Fig. 10. Electrochemical impedance spectra of 20 wt% and 40 wt% Si on Ni and 20 wt% Si on Cu.

that the charge transfer resistance with Ni foam as the current collector is much lower than that with Cu foil because of the good electrical connection of 3D structure. Also the electrode with 20% Si and Ni foam shows lowest impedance, which corresponds to the best cycle life.

4. Conclusions

The structural properties of electrode substrates should be sufficiently considered prior to the application as a current collector. In this study, through a detailed comparison experiment of Cu and Ni current collectors, the network geometry of nickel foam displays an improvement of the cycle life of silicon based anode. The network can support larger weight percent of silicon, which is really helpful for the improvement of lithium ion battery. It is also shown that the flatness and smoothness of copper foil should be responsible for the anode material crack and drop off from the current collectors after completely dried. In the end, among the three battery models, the Si anode on Ni has the smallest impedance, and this is another important aspect of Ni current collector. Therefore, adopting 3D current collector provides a new way to incorporate electrode materials with large volume expansion.

Acknowledgments

The authors thank Worcester Polytechnic Institute for the startup financial supporting. Qina Sa acknowledges the financial support from Helen E. Stoddard Fellowship.

References

- [1] K. Kinoshita, K. Zaghbi, J. Power Sources 110 (2002) 416–423.
- [2] R.A. Huggins, in: J.O. Besenhard (Ed.), Handbook of Battery Materials, Wiley/VCH, Weinheim, 1999, p. 359.
- [3] J.O. Besenhard, J. Yang, M. Winter, J. Power Sources 68 (1997) 87–90.
- [4] J.M. Tarascon, M. Armand, Nature 414 (2001) 359–367.
- [5] R.A. Huggins, J. Power Sources 81–82 (1999) 13–19.
- [6] C.J. Wen, R.A. Huggins, J. Solid State Chem. 37 (1981) 271–278.
- [7] J.P. Maranchi, A.F. Hepps, A.G. Evans, N.T. Nuhfer, P.N. Kumta, J. Electrochem. Soc. 153 (2006) A1246–A1253.
- [8] H. Li, X. Huang, L. Chen, Z. Wu, Y. Liang, Electrochem. Solid State Lett. 2 (1999) 547–549.
- [9] C.S. Wang, G.T. Wu, X.B. Zhang, Z.F. Qi, W.Z. Li, J. Electrochem. Soc. 145 (1998) 2751–2758.
- [10] M. Chhowalla, K.B.K. Teo, C. Ducati, N.L. Rupasinghe, G.A.J. Amaratunga, A.C. Ferrari, D. Roy, J. Robertson, W.I. Milne, J. Appl. Phys. 90 (2001) 5308–5317.
- [11] M. Yoshio, H. Wang, K. Fukuda, T. Umeno, N. Dimov, Z. Ogumi, J. Electrochem. Soc. 149 (2002) A1598–A1603.
- [12] X.Q. Wang, J. McBreen, W.-S. Yoon, M. Yoshio, H. Wang, K. Fukuda, T. Umeno, Electrochem. Commun. 4 (2002) 893–897.
- [13] C.K. Chan, H. Peng, G. Liu, K. McIlwrath, X. Zhang, R.A. Huggins, Y. Cui, Nat. Nanotechnol. 3 (2008) 3–35.
- [14] M. Yoshio, S. Kugino, N. Dimov, J. Power Sources 153 (2006) 375–379.
- [15] N. Dimov, S. Kugino, M. Yoshio, Electrochim. Acta 48 (2003) 1579–1587.
- [16] I. Kovalenko, B. Zdyrko, A. Magasinski, B. Hertzberg, Z. Milicev, R. Burtovyy, I. Lutzenov, G. Yushin, Science 334 (2011) 75–79.
- [17] G.-B. Cho, B.-K. Lee, W.-C. Sin, K.-K. Cho, H.-J. Ahn, T.-H. Nam, K.-W. Kim, J. Mater. Sci. 41 (2006) 313–315.
- [18] K.L. Lee, J.Y. Jung, S.W. Lee, H.S. Moon, J.W. Park, J. Power Sources 129 (2004) 270–274.
- [19] T. Sakai, I. Uehara, H. Ishikawa, J. Alloys Compd. 293–295 (1999) 762–769.